SUB-GRID SCALE OROGRAPHIC GRAVITY WAVE DRAG AND MOUNTAIN BLOCKING AT NCEP

Jordan C. Alpert

Physics Component Training

Q3FY2018

June 13, 2018

Outline

- Mountain Blocking
- Orographic Gravity Wave Drag (including TOFD)
- Convective Gravity Wave Drag
- Unified GW with Non-orographic GWD

- Gravity waves from water vapor images

Correction of Model Bias from Sub-grid Scale Processes

Atmospheric flow is significantly influenced by orography, creating lift and frictional forces.

The representation of orography and its influence in numerical weather prediction models are necessarily divided into resolvable scales of motion and treated by primitive equations, the remaining sub-grid scales to be treated by parameterization.

Orographic Gravity wave Drag, 1987, 1997
Mountain Blocking, 2004
Upgrade including Vertical Diffusion, 2005
Convective Gravity Wave Drag, 2014

Mountain blocking of wind flow around sub-grid scale

Flow around the mountain encounters larger frictional forces by being in contact with the mountain surfaces for longer time as well as the interaction of the atmospheric environment and vortex shedding which is shown to occur in numerous observations and tank simulations.

Correction of Model Bias from Sub-grid Scale Processes Mountain Blocking

- Lott and Miller (1997) incorporated the dividing streamline where above the dividing streamline, gravity waves are potentially generated and propagate vertically, and below, the flow is expected to go around the barrier with increased friction in low layers.

- The idea of a dividing streamline at some level, h_d, dividing air parcels that go over the mountain from those forced around an obstacle is used to parameterize mountain blocking effects.
- Recent studies of model behavior have shown that models underestimate mountain drag. Further, the NWP models generate mountain disturbances which have horizontal scales that are the same as the model truncation.

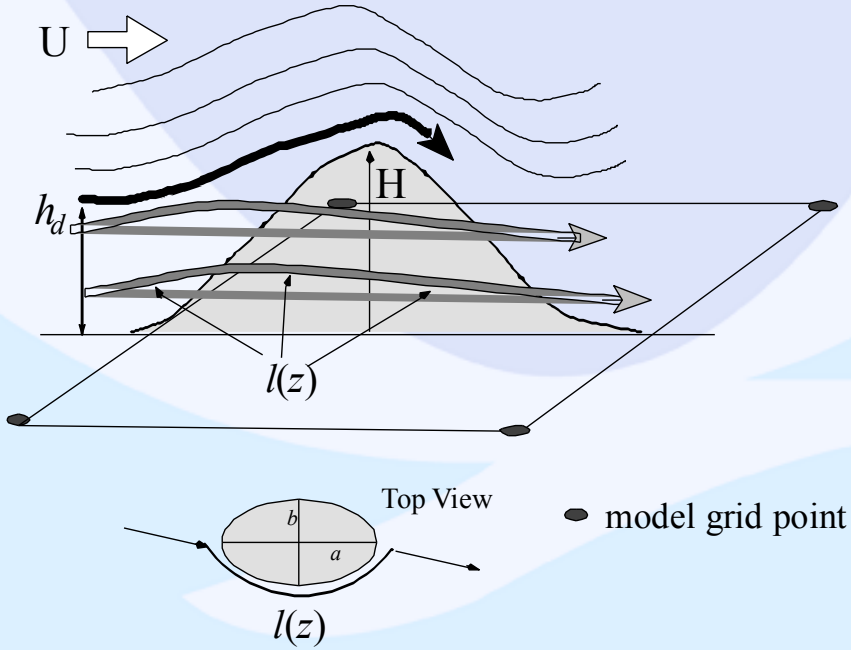

Fig 1. Representationof the low-level flow above and below the dividing streamline.

Mountain Blocking

The dividing streamline height, of a sub-grid scale obstacle, can be found from comparing the potential and kinetic energies of up stream large scale wind and sub-grid scale air parcel movements. These can be defined by the wind and stability as measured by N, the Brunt Vaisala frequency. The dividing streamline height, h_d, can be found by solving an integral equation for h_d:

$$U^2(h_d) = \int_{h_d}^{H} N^2(z)(H - z)dz$$

where H is the maximum elevation within the sub-grid scale grid box of the actual orography, h, from the GTOPO30 dataset of the U.S. Geological Survey.

In the formulation, the actual orography is replaced by an equivalent elliptic mountain with parameters derived from the topographic gradient correlation tensor, H_{ij}:

$$H_{ij} = \overline{\frac{\partial h}{\partial x_i}} \overline{\frac{\partial h}{\partial x_j}}$$

The model sub-grid scale orography is represented by four parameters, after Baines and Palmer (1990), h', the standard deviation, g, s, Q, the anisotropy, slope and geographical orientation of the orography form the principal components of H_{ij}, respectively. These parameters will change with changing model resolution (Orog_maker: USGS 30” elevations).

The length scale function, *l(z) in the Dissipation*:

$$D_d(z) = -\rho C_d l(z) U|U|/2 \qquad (1) \qquad (2) \qquad (3)$$

$$l(z) = \max(2 - 1/r, 0) \times \frac{\sigma}{2h'} \sqrt{\left[\frac{h_d - z}{z + h'}\right]} \max(\cos\psi, \gamma \sin\psi)$$

Term (1) relates the eccentricity parameters, a,b, to the sub-grid scale orography parameters (Fig. 1), *a ~ h'*s and *a/b* = g and allows the drag coefficient, C_d to vary with the aspect ratio of the obstacle, as seen by the incident flow, since it is twice as large for flow normal to an elongated obstacle compared to flow around an isotropic obstacle.

Term (2) accounts for the width and summing up a number of contributions of elliptic obstacles, and

Term (3) takes into account the flow direction in one grid region.

Some of the motivation for applying the sub-grid scale MB is models reduced bias and RMS errors by adding an orography enhancement such as enhanced mountains or "silhouette" mountains. Anomaly Correlation (NH 20-80N) skill for enhanced orography is shown for a low resolution experiment.

But then the elevation of the models surface and interaction with observations became a problem.

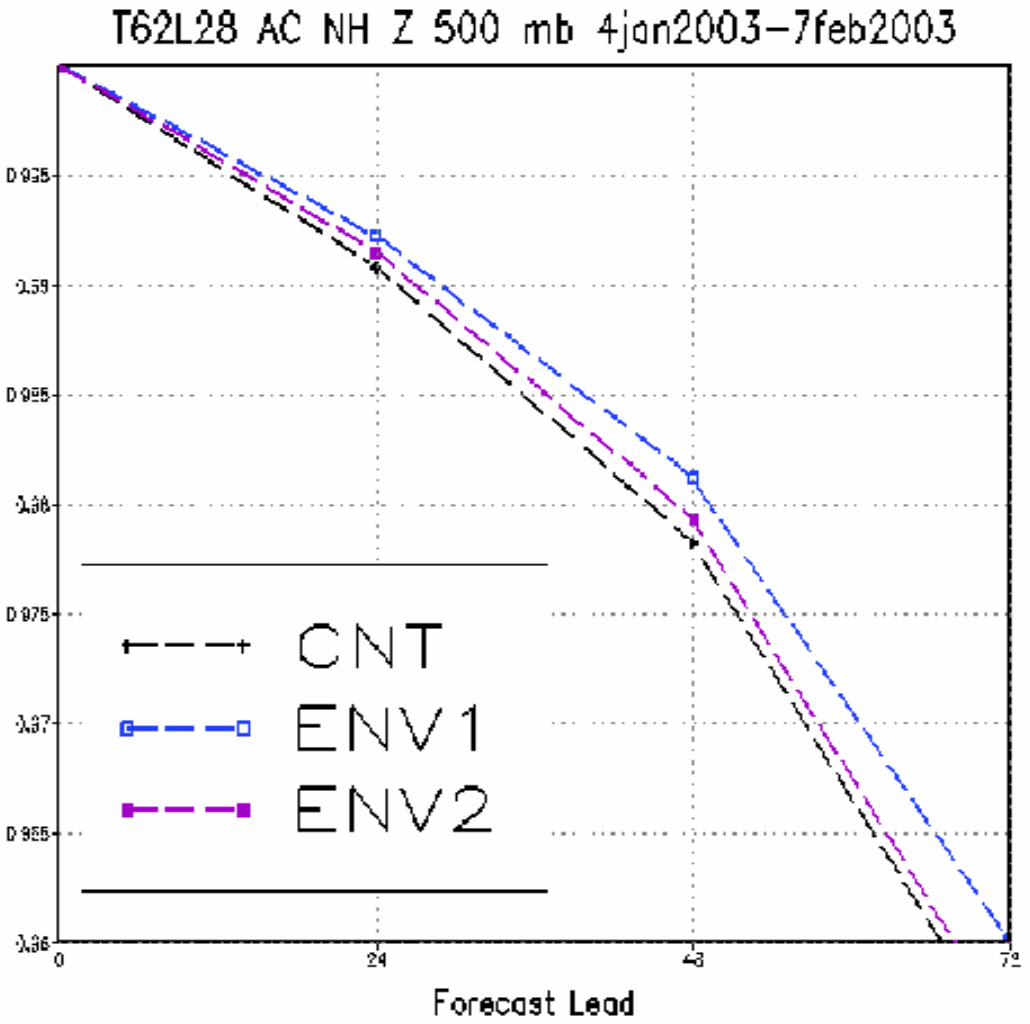

⇒ As noted in a number of studies of model behavior (Lott and Miller, 1977), the mountain drag is underestimated. Traditionally models responded to orography enhancements to correct this problem:

In Kim, Moorthi, Alpert's (1998, 2001) GWD

This GWD scheme has the same physical basis as in Alpert (1987) with the addition of enhancement factors for the amplitude, G, and mountain shape details to account for some effects from the mountain blocking,

$$\tau_x = E\frac{m'}{\Delta x}\varrho\,\frac{U^3}{N}G(F_r) \qquad (1K)$$

E is an enhancement factor over the stress in the Alpert '87 scheme. It ranges from no enhancement to an upper limit of 3, E=E(OA)[1−3]. E is a function of OA, the Orographic Asymmetry defined in KA (1995) as

$$\text{Orographic Asymmetry (OA)} \equiv \frac{\bar{x} - \sum_{j=1}^{N_B} x_j n_j}{\sigma_x} \qquad (2K)$$

In Alpert GWD (1987)

Based on linear, two−dimensional non−rotating, stably stratified flow over a mountain ridge, gravity wave motions are set up which propagate away from the mountain. The flux measured over a "low level" vertically averaged layer, in the atmosphere defines a base level flux. "Low level" was taken to be the first 1/3 of the troposphere in the 1987 implementation but this choice was arbitrary. This remained in operations for 10 years when it was augmented with Kim's scheme in 1997. The vertical momentum flux or gravity wave stress in a grid box due to a single mountain is given as in PH:

$$\tau_x = \varrho\ U^3\frac{G(F_r)}{N\ \Delta x} \qquad (1A)$$

where $\sum L_h/\Delta x \equiv L_x$, is the fractional area covered by the subgrid–scale orography higher than a critical height ($h_c \equiv Fr_c U_0/N_0$) for a grid box with the interval, Δx. Each L_h is the width of a segment of orography intersection at h_c.

$$Fr_0 = N_0 h'/U_0 \qquad a^2 = \frac{C_G}{OC}$$

$$G'(OC, Fr_0) = \frac{{Fr_0}^2}{\left({Fr_0}^2 + a^2\right)} \qquad (5K)$$

$$E(OA, Fr_0) = (OA + 2)^{\delta}$$

$$\delta = \frac{C_E Fr_0}{Fr_c}$$

where Fr_c is as in Alpert.

$$\textit{Orographic Convexity (OC)} \equiv \frac{\sum_{j=1}^{N_x} \left(h_j - \bar{h}\right)^+}{N_x \sigma_h^+}$$

$$\sigma_h \equiv \sqrt{\frac{\sum_{j=1}^{N_x} \left(h_j - \bar{h}\right)^2}{N_x}}$$

giving the stress in a grid box. PH gives the form for the function $G(F_r)$ as

$$G(Fr) = \overline{G}\frac{Fr^2}{\left(Fr^2 + a^2\right)} \qquad (5A)$$

where $\overline{G}$ is an order unity non–dimensional saturation flux set to 1.0 and 'a' is a function of the mountain aspect ratio also set to 1 in the 1987 implementation. Typical values of U=10m/s, N=0.01s^{-1}, l^* = 100 km, give a flux of 1 Pascal. If this flux goes to zero linearly with height, then the deceleration would be 10m/s, which is consistent with observations. In Fig. 1, the flux function, $G(F_r)$, is shown as a function of Froude number and mountain shape parameters a^2=0.5, 1.0, 1.5. A value of 1.0 for 'a' was used in the 1987 implementation.

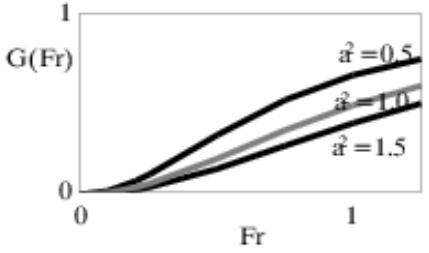

Fig. 1. Universal flux function, G.

Orographic GWD vs Convective GWD

Kim, Moorthi & Alpert's vs Chun and Baik's CGWD developed by Ake
Both based on linear, 2-D non-rotating, stably stratified Homogenous vs non-Homogenous flow

- $\tau = E\ \frac{m}{\Delta x}\left\{\rho\ \frac{U^3}{N}\ \mathrm{G}(F_r)\right\}$; Alpert's version $\hat{G}\&a = 1, and\ E\ \frac{m}{\Delta x}\ constant\ but$ KMA
- $G(F_r) = \hat{G}\ \frac{{F_r}^2}{(Fr^2+a^2)}$, $F_r = \mathrm{N}\acute{h}/U$; has $E\ \frac{m}{\Delta x}$ and **a** from GW model stats.
- $\tau = \rho\ \frac{U^3}{N}\ \mathrm{G}(F_r)$; Ake's (C&B) adds (gQ/cpT0) to the vertical GW equation
- $G(F_r) = c_1\ {c_2}^2\ \mu^2$; resulting in convection induced momentum flux.
- $\mu = gQ_0a_1/\left(c_pT_0\mathrm{N}U^2\right)$; Where a1 is related to structure of thermal forcing, c2 to the basic-state wind and stability and the bottom and top heights of thermal forcing making up a nonlinearity factor of thermally induced gravity waves, (C&B, 1994).

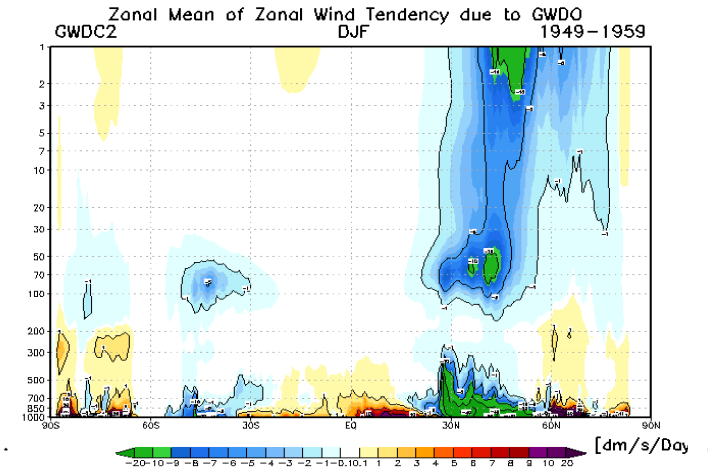

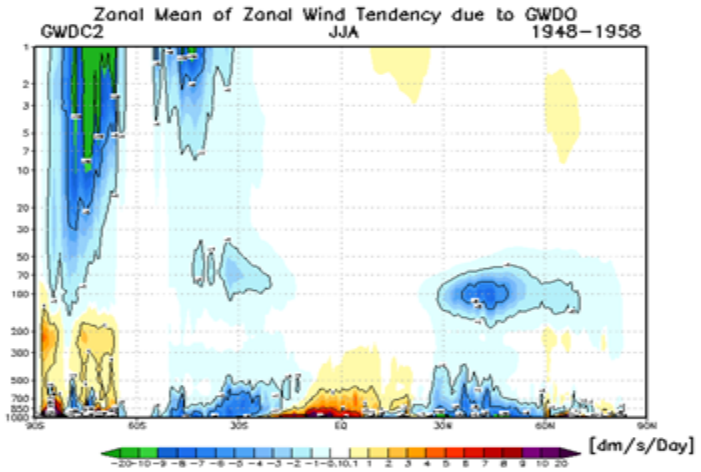

Climatological mean of the tendency of the zonal mean zonal wind due to **orographic gravity wave drag**. Left panel is for boreal winter and right panel for boreal summer. Unit is **dm/s/Day**.

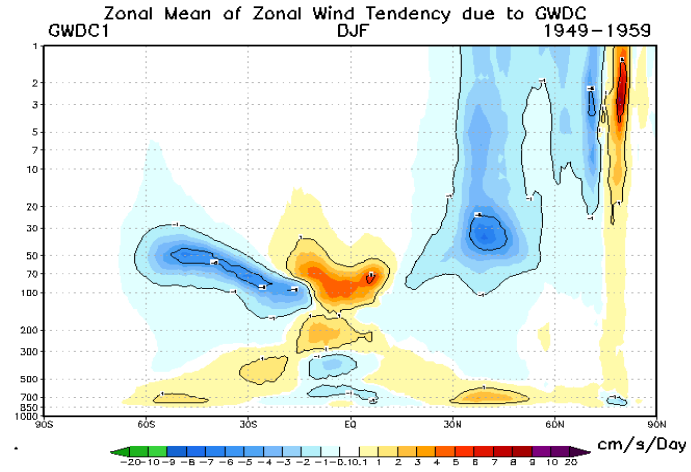

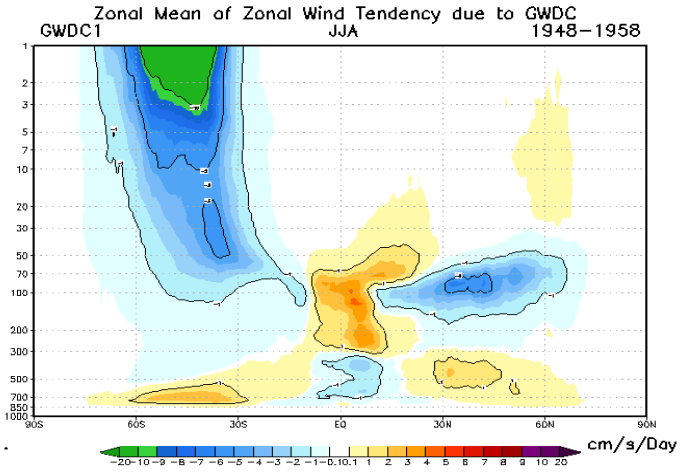

Zonal mean of zonal wind tendency due to C**GWD** in units of **cm/s/Day**

… from Ake's presentation.

Skill Score	AC H500 NH		AC H500 SH	
Experiment \ Season	DEC-JAN	JUL-AUG	DEC-JAN	JUL-AUG
CNTR	**87.0**	**81.3**	**84.1**	**80.0**
GWDC2	**87.4**	**81.4**	**83.9**	**79.9**
GWDC2-CNTR	**0.4**	**0.1**	**-0.2**	**-0.1**

Skill scores for **GWDC**

Mountain Blocking: The Regional Spectral Model (RSM) has the same physical parameterization as the GFS but is run at 10 km resolution over Hawaiian islands so it is useful to compare simulations as a proxy for the events to be modeled. The RSM is initialized by the GFS which responds weakly to the presence of the barriers.

By 21Z, 9-h later, the RSM (right) shows streamlines and wind barbs bending around the big island with a wind shadow on the lee side. The wind speeds show that 20 knot winds are reduced to near zero and reverse in the shadow zone. The surface pressure increases on the windward side and decreases on the leeward side and increased wind speeds are seen along the lateral sides of the barrier. The vorticity responds to the jets and soon sheds vortices down stream of the barrier. Note the similarity between the big Island and Maui, the closest but smaller island as the GFS is to the RSM.

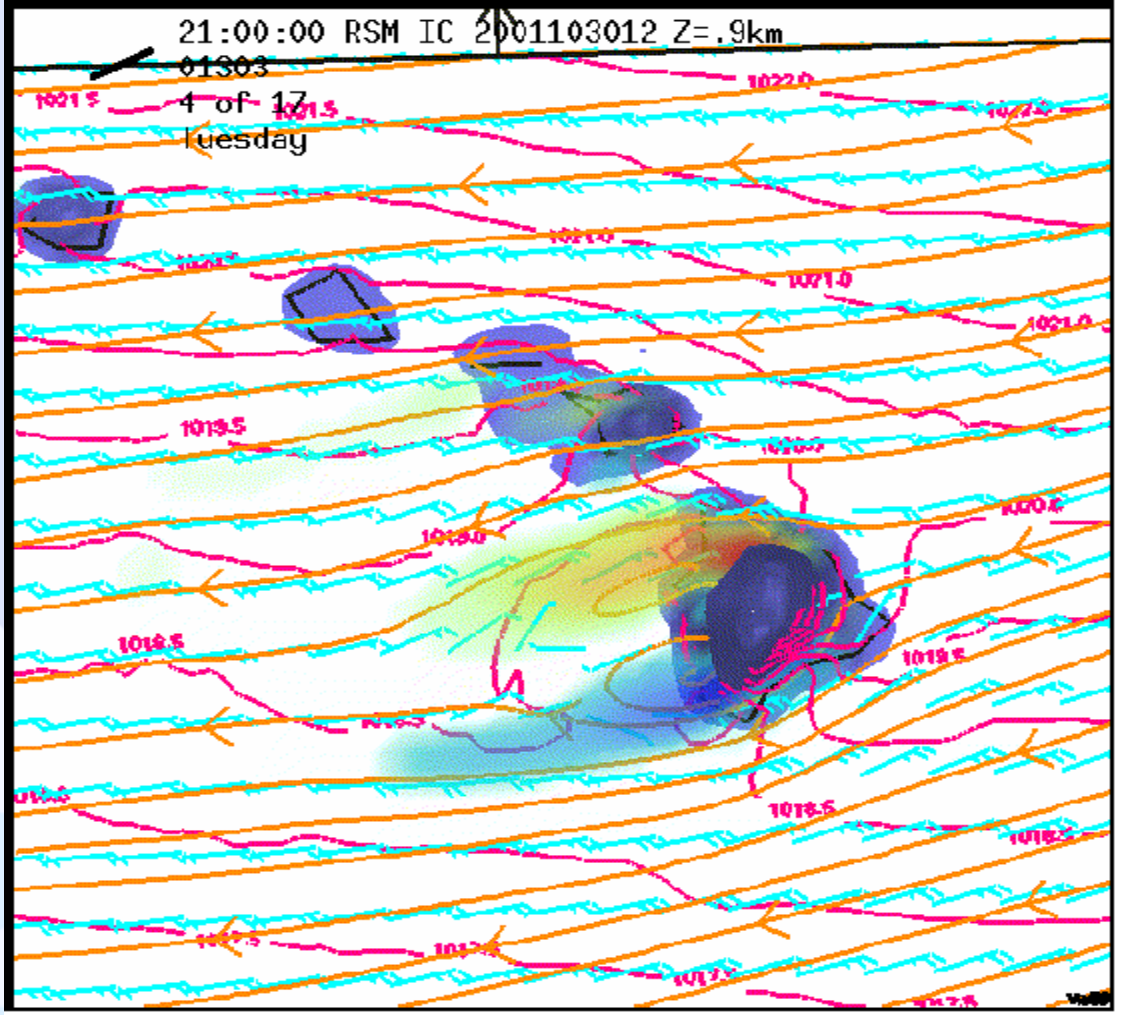

Fig 2. The NCEP 10km RSM initial condition (f00) 2001103012 from the GFS 1x1 degree (left) and a 9 hour forecast (right). Streamlines in Orange, Wind Barbs (knots) in Blue, Surface pressure (0.5 mb) in red and Absolute Vorticity above 10E-04/sec shaded in reds and below -10E-04/sec shaded in Blues, all at 0.9 km.

Model skill scores at low resolution show impressive gains in anomaly correlation and RMS errors.

The improvement in scores in low resolution experiments are not as large in the high resolution. Mountain Blocking is consistently an improvement.

Periodically a number of runs are done to test calibration of the vertical diffusion and MB/GWD.

The Turbulent Orographic Form Drag (TOFD) is handled by Kim's enhancement as TOFD and GWD are functions of elevation variance and calculations show (Toy, et al 2018) horizontal distribution is very similar, so amplitude can be adjusted.

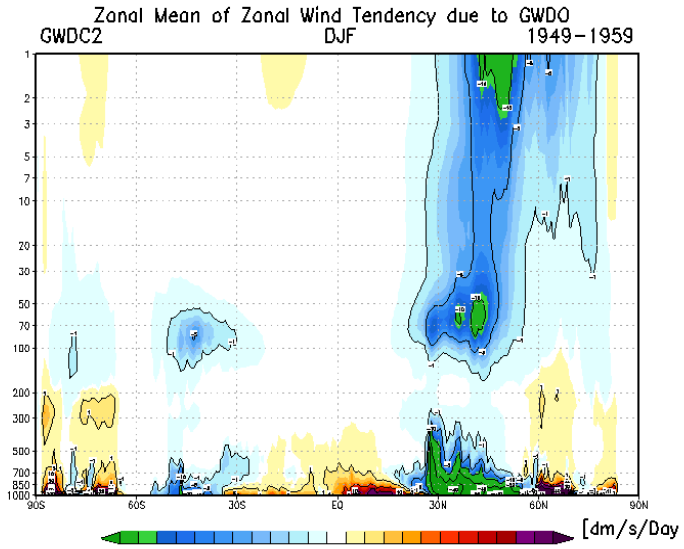

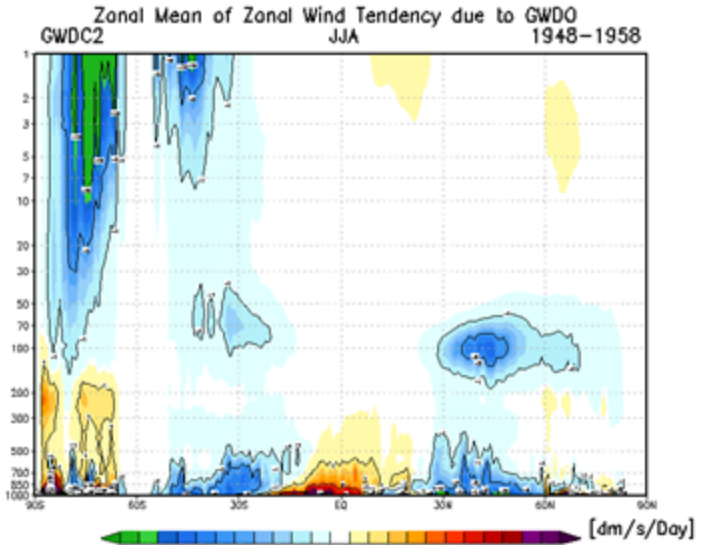

Climatological mean of the tendency of the zonal mean zonal wind due to **orographic gravity wave drag**. Left panel is for boreal winter and right panel for boreal summer. Unit is **dm/s/Day**.

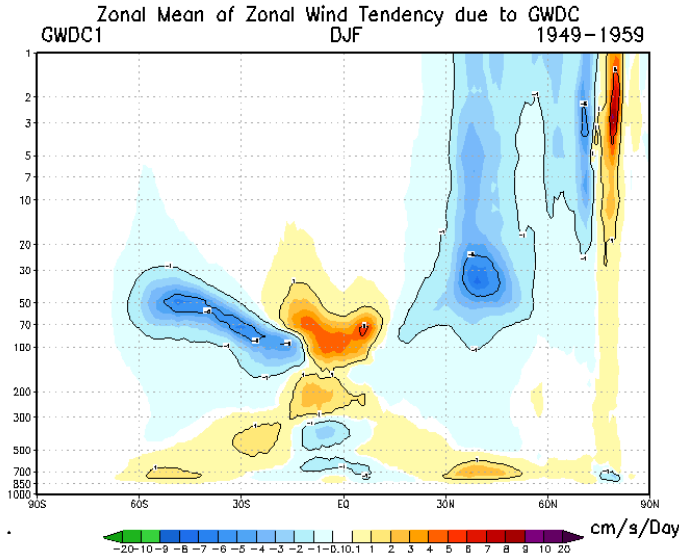

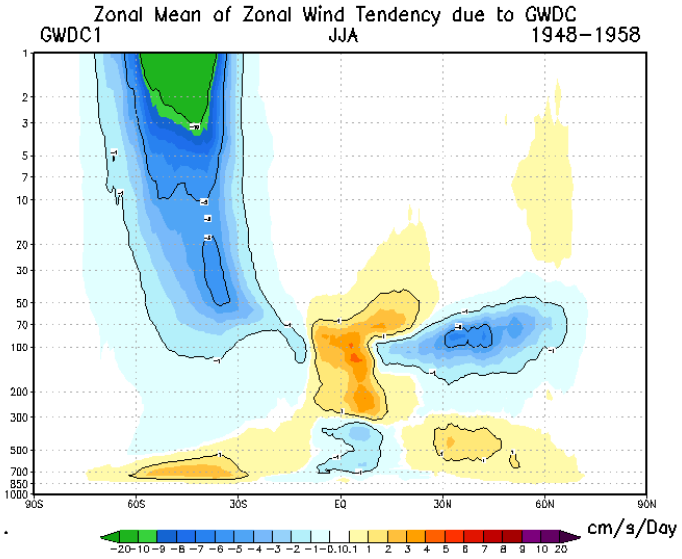

Zonal mean of zonal wind tendency due to **GWDC** in units of **cm/s/Day**

SLIDES taken from Ake's presentation.

Skill Score	AC H500 NH		AC H500 SH	
Experiment \ Season	DEC-JAN	JUL-AUG	DEC-JAN	JUL-AUG
CNTR	**87.0**	**81.3**	**84.1**	**80.0**
GWDC2	**87.4**	**81.4**	**83.9**	**79.9**
GWDC2-CNTR	**0.4**	**0.1**	**-0.2**	**-0.1**

Skill scores for **GWDC**

The existence of the QBO is due to wave-mean flow interactions in the tropical stratospheres. The waves that participate in these interactions, large scale Kelvin and Rossby-gravity waves as well as smaller scale internal gravity waves, all have non-zero phase speeds. Because of the importance of non-stationary gravity waves, not only for the QBO but also in general, a second class of parameterization schemes has been developed where a gravity-wave spectrum is assumed which includes both stationary waves and waves of varying phase speeds.

Next Steps:

- Test non-orographic GWD spectrum
  (ECMWF and NCAR approach's are candidates)
- Test sub grid scale effects from form drag (<5km) as in ECMWF
- Unifiy GWD project (uGWD w/ Valery Yudin)
- Test including GWD contributions as additions to diffusion (MONIN)
  (code speed up and enable reduction in diffusion)
- uGWD with non-stationary waves
  Merging WAM physics under Physics_layer

GWD and MB code

Source code name for the convective gravity wave drag
cgwd_drv.f driver and subroutine gwdc.f

Source code name for the orographic gwd and mountain blocking
gwdps.f

Namelist parameters:
Multiplierfor Mtn Blocking: cdmbgwd(1)
Multiplyer for GWD: cdmbgwd(2)

MTNVAR14

1. Variance
2. Var4; Kim's 4th moment
3. OA1: Kim's Orographic Asymmetry
4. OA2: "
5. OA3: "
6. OA4: "
7. OL1: Kim's Orographic convexity
8. OL2: "
9. OL3: "
10. OL4: "
11. THETA : Angle of mountain
12. GAMMA: Asymmetry
13. SIGMA : Slope
14. ELVMAX: Max elevation

References

Alpert, J.C., S-Y Hong and Y-J Kim, 199x: Sensitivity of cyclogenesis to lower troposphere enhancement of gravity wave drag using the Environmental Modeling Center medium range model.

Alpert, J.C., M. Kanamitsu, P.M. Caplan, J.G. Sela, G.H. White, and E. Kalnay, 1988: Mountain induced gravity wave drag parameterization in the NMC medium-range model. Preprints of the Eighth Conference on Numerical Weather Prediction, Baltimore, MD, American Meteorological Society, 726-733.

Kim, Y-J and A. Arakawa, 1995: Improvement of orographic gravity wave parameterization using a mesoscale gravity wave model. J. Atmos. Sci. 52, 11, 1875-1902.

Lott, F and M. J. Miller: 1977, A new sub-grid scale orographic drag parameterization: Its formulation and testing, QJRMS, 123. pp101-127.

Baines, P.G. and Palmer, T.N., 1990: Rationale for a new physically based parameterization of sub-grid scale orographic effects, Tech. Mem. #169. ECMWF.

Background Slides

- Lott and Miller (1997) incorporated the dividing streamline into the ECMWF global model, as a function of the stable stratification, where above the dividing streamline, gravity waves are potentially generated and propagate vertically, and below, the flow is expected to go around the barrier with increased friction in low layers.
- An augmentation to the gravity wave drag scheme in the NCEP global forecast system (GFS), following the work of Alpert et al., (1988, 1996) and Kim and Arakawa (1995), Mountain Blocking is incorporated from the Lott and Miller (1997) scheme including the dividing streamline.

In each model layer below the dividing streamline a drag from the blocked flow is exerted by the obstacle on the large scale flow and is calculated as in Lott and Miller (1997):

$$D_d(z) = -\rho C_d l(z) U|U| / 2$$

where *l(z)* is the length scale of the effective contact length of the obstacle on the sub grid scale at the height z and constant $C_d \sim 1$.

$$l(z) = F(z, h_d, h', g, s, Q, ?)$$

Where $? = Q - ?$, the geographical orientation of the orography minus the low level wind vector direction angle, *?*.

$$\frac{\tau_i}{\tau_{i+1}} = \min\left[C_l \frac{l_i^2}{l_{i+1}^2}, 1\right]$$

where Cl=1 and l^2 is given by:

$$l^2 \equiv \frac{N^2}{U^2} - S^2/4 - \gamma/U,$$

where the buoyancy N, the heterogeneity S, and the vertical wind curvature, γ, are defined by (2A) and:

$$S \equiv -\frac{d \ln \varrho_0(z)}{dz} \qquad \gamma \equiv \varrho_0 \frac{d\left[(1/\varrho_0) dU/dz\right]}{dz}$$

Since S and γ generally may not change compared to N/U, and sub–grid scale observations are not very accurate, the difference between this and Alpert may not be large.

$$Fr_c = N\frac{h_c}{U} = 1 - \frac{1}{4Ri} \qquad (7A)$$

where h_c is the critical vertical displacement amplitude for a wave in the free atmosphere which is about to break. This means that a shear instability is assumed to occur at Ri<1/4. The criteria for shear instability is difficult to determine and convective breaking (Ri<0) criterion is usually satisfied before that of shear breaking. Both of the above criteria are used in the present parameterization. However, if Ri<0 occurs in the base level, then no deposition takes place.

where N_b is the totol number of bottom blocks in the barrier, σ_x is the standard deviation of the horizontal distance defined by

$$\sigma_x \equiv \frac{1}{N_x}\sum_{j=1}^{N_x}\left(x_j - \bar{x}\right)^{1/2} \qquad (3K)$$

where N_x the number of grid intervals for the large scale domain being considered. So the term, $E(OA)m'/\Delta x$ in Kim's (1) represents a multiplier on $\bar{G}$ in Alpert's eq (1).

Where m' was the number of mountains in a sub–grid scale box in Alpert's scheme, it is now a more complex function of the fractional area of the the subgrid mountain and the asymmetry and convexity statistics as shown.

$$m' = C_m \Delta x \left[1 + \frac{\sum_x L_h}{\Delta x}\right]^{OA+1} \qquad (4K)$$

where Δx is a grid increment, N is the Brunt Viasala frequency

$$N(\sigma) = \frac{-g^2\sigma\frac{\partial\theta}{\partial\sigma}}{\theta RT} \qquad (2A).$$

The environmental variables are calculated from the mass weighted vertical average over the base layer. Shown in eqn. (4A), G(Fr) is a monotonically increasing function of Froude number,

$$Fr = Nh'/U \qquad (3A)$$

where U is the wind speed calculated as a mass weighted vertical average in the base layer, and h', is the vertical displacement caused by the orography variance. An effective mountain length, $l^* = \Delta x/m$ where m is the number of mountains in a grid box, can then be defined to obtain the form of the base level stress

$$\tau = \varrho\frac{U^3}{Nl^*}\,G(Fr)\,, \qquad (4A)$$

giving the stress in a grid box. PH gives the form for the function $G(F_r)$ as

Typical values of parameters:

$OA:[-1,1]; L_x:[0,1]; C_{m\,\Delta x=1\ and}\quad \delta = 1$

given for C_E, C_M, and C_G constants to be specified, for example:

$C_E=0.8$, $C_M=3.3X10^{-5}m^{-1}$ and $C_G=0.5$ for $m < \Delta x/L_m = 50$ km/20 km.

Wave breaking occurs when the minimum Richardson number $R_{im} < R_{ic}=0.25$, and determined by:

$$Ri_m = \frac{Ri\left(1-F_{r_d}\right)}{\left(1+\sqrt{Ri}F_{r_d}\right)^2}$$

Which is approximately the same criteria as in Alpert (6A). when the denominator is near order 1 or equivalently Froude and Richardson numbers are small, the same criteria required for the saturation hypothesis. The saturation hypothesis in Kim's scheme uses a ratio of Scorer parameters on adjacent vertical levels:

When breaking occurs for some layer in the free atmosphere the stress at the next lower layer is known starting with the base level flux described in (5). This representation of the stress in (5), under a binomial expansion for small Froude number, is identical to that used in the free atmosphere:

$$\tau = \varrho\ U\ N\ k\ h'^2 \qquad (6A)$$

with $l^* = 1/k$, where k is an inverse length scale parameter given as $2.5x10^{-5}\ m^{-1}$ noting: $(1+x)^{-1} = 1-x+O(x^2)$ so for *small* F_r, $G(F_r)$ becomes

$$\overline{G}\frac{Fr^2}{(Fr^2+a^2)} = \frac{\overline{G}Fr^2}{a^2}\left(\frac{1}{1+\frac{Fr^2}{a^2}}\right) =$$

$$\overline{G}\frac{Fr^2}{a^2}\left(1-\frac{Fr^2}{a^2}+O\left(\frac{Fr^2}{a^2}\right)^2\right) = \overline{G}\frac{Fr^2}{a^2}$$

if terms of less than second order are considered. Then (6A) and (4A) are approximately equal.

Wave breaking occurs at the level where the amplification of the wave causes the local Froude number to exceed the critical value

Averaging 7 cycles of 5 day forecasts of the T254 GFS over Hawaii to compare with the RSM in Fig 2.

Wind Difference (contours, [m/s]) of mountain blocking (MB) minus operational GFS from an average of 7 forecast experiments with independent cycling analysis of Observations. The model orography ("what the model sees") is shown in Blue and the total wind is shown in Green vectors with a prevailing flow of ~12 m/s. The wind difference vectors are in Red (max 1 m/s): An east red vector indicates the wind is reduced in the experiment and a westward pointing red vector shows an increase in the MB wind.

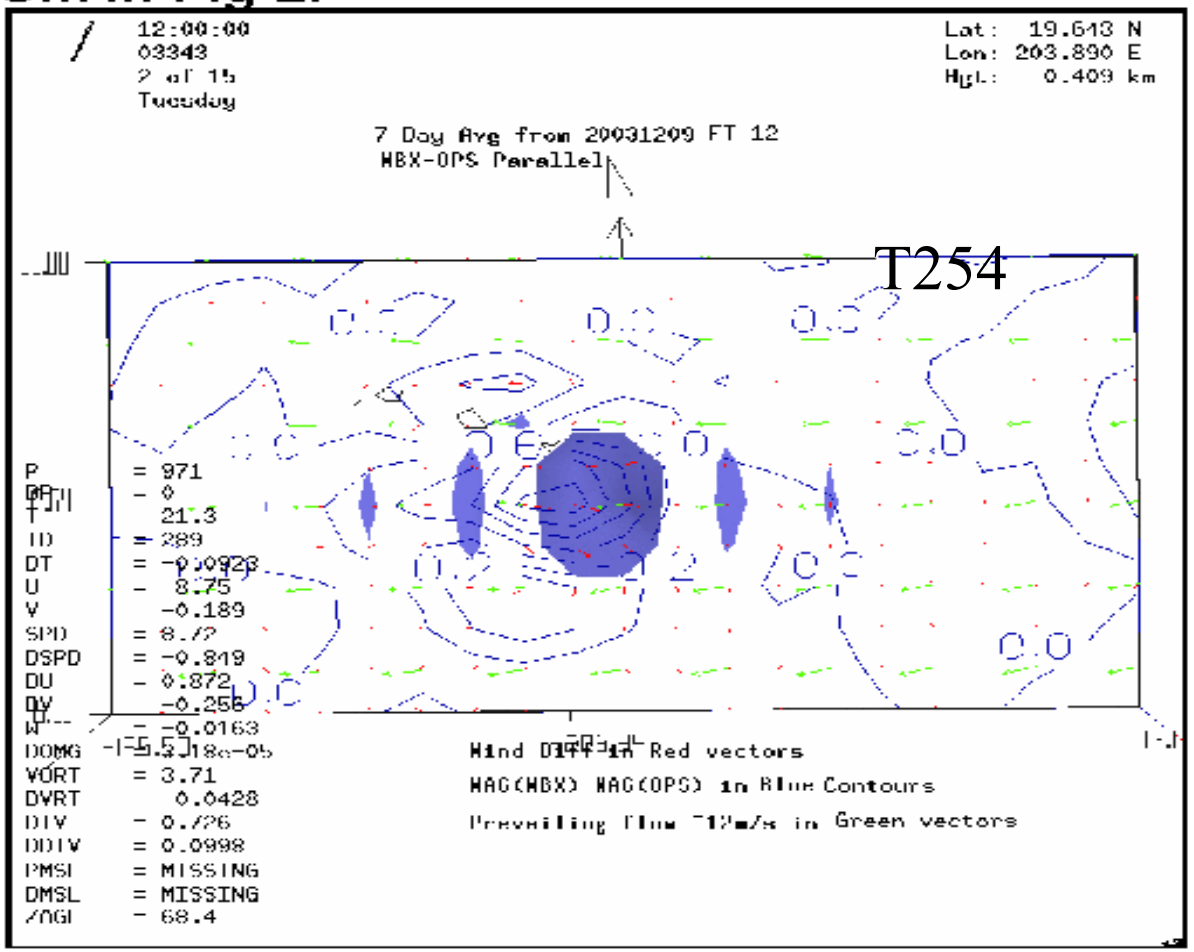

Fig 3. Wind difference (contours, m/s) of mountain blocking (MB) minus operational GFS from and average of 7 forecast experiments with independant cycling analysis of observations. The model orography ("what the model sees") is shown in in blue and the total wind is shown in Green vectors with a prevailing flow of ~12 m/s. The wind difference vectors are in red (max 1 m/s): An east red vector indicates the wind is reduced in the MB experiment and a westward pointing red vector shows and increace in the MB wind.